JPE 16-3-16

http://dx.doi.org/10.6113/JPE.2016.16.3.982
ISSN(Print): 1598-2092 / ISSN(Online): 2093-4718

Performance Evaluation of the Field-Oriented Control of Star-Connected 3-Phase Induction Motor Drives under Stator Winding Open-Circuit Faults

Mohammad Jannati*, Nik Rumzi Nik Idris†, and Mohd Junaidi Abdul Aziz*

*,†UTM-PROTON Future Drive Laboratory, Faculty of Electrical Engineering, Universiti Teknologi Malaysia, Johor Bahru, Malaysia

Abstract

A method for the fault-tolerant vector control of star-connected 3-phase Induction Motor (IM) drive systems based on Field-Oriented Control (FOC) is proposed in this paper. This method enables the control of a 3-phase IM in the presence of an open-phase failure in one of its phases without the need for control structure changes to the conventional FOC algorithm. The proposed drive system significantly reduces the speed and torque pulsations caused by an open-phase fault in the stator windings. The performance of the proposed method was verified using MATLAB (M-File) simulation as well experimental tests on a 1.5kW 3-phase IM drive system. This paper experimentally compares the operation of the proposed fault-tolerant vector controller and a conventional vector controller during open-phase fault.

Key words: Fault-tolerant control, Field-Oriented Control (FOC), Speed and torque pulsations, Star-connected, Stator winding open-circuit fault, 3-phase induction motor drive

I. INTRODUCTION

The Field-Oriented Control (FOC) technique for 3-phase Induction Motors (IMs) is widely adopted by industries to obtain high performance from 3-phase IM drive systems. The conventional FOC algorithm, which is used for healthy 3-phase IM drives, cannot be used for a faulty 3-phase IM drive due to the fact that the conventional FOC was designed based on a healthy machine model [1]. Using the conventional FOC for faulty 3-phase IM drives will degrade the dynamic performance of drive systems. In this regard, it is necessary to design a drive system that provides robustness against fault conditions [1]-[5].

Generally, 3-phase IM drives are exposed to various failures including failures in the in the inverter [6], [7], failures in the mechanical or electrical sensors [5], [8] and failures related to the electrical motor including faults in the stator [1], [9] and/or faults in the rotor [10], [11]. Fig. 1 shows the classification of faults in squirrel-cage 3-phase IM drives. In some critical applications, the operation of the drive system cannot be interrupted by faulty conditions for mainly safety reasons. Thus, for these applications, fault-tolerant control is essential. Based on this classification of faults, various fault-tolerant control methods have been suggested in the literature including both passive and active methods. A passive method can be ensured by conventional robust control methods such as the H_∞ [12], [13]. Despite the robustness of this method against disturbances, its performance under healthy conditions is not optimized. In active methods after fault detection and fault diagnosis, a new set of control parameters or a new control structure is applied [1]-[5] and [14]-[20]. These methods have good performances under both healthy and faulty conditions. However, they requires a different control algorithm under faulty conditions.

A large number of studies have been conducted on the implementation of vector control techniques for electrical machines under stator open-circuit faults [1]-[4] and [14]-[20]. Most of these works focused on developing vector control methods of faulty Permanent Magnet Synchronous Motors (PMSMs) and multi-phase IMs (five and six phase) [14]-[17]. In [18], [19] the analysis of star-connected 3-phase IMs in an

Manuscript received Jun. 12, 2015; accepted Oct. 8, 2015
Recommended for publication by Associate Editor Dong-Hee Lee.
†Corresponding Author: nikrumzi@fke.utm.my
Tel: +6075536139, Universiti Teknologi Malaysia
*UTM-PROTON Future Drive Laboratory, Faculty of Electrical Engineering, Universiti Teknologi Malaysia, Malaysia

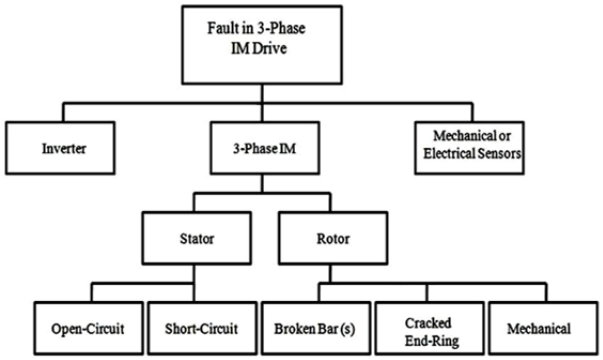

Fig. 1. Classification of faults in squirrel-cage 3-phase IM drive.

open-phase fault indicates that the odd harmonic voltages of the magnitude and phase angle can be injected at the machine terminal to compensate torque pulsations. In [3], [20], vector and scalar control methods to control delta-connected 3-phase IM drives under a stator winding open-phase fault based on a current controller has been proposed and implemented. The modeling and FOC of a star-connected 3-phase IM under open-phase fault using a current controller has also been presented in [4]. In this study, by using a suitable transformation matrix for the stator current variables, a new model of an IM is adopted during faulty conditions. This method is only verified by simulation results. Moreover, the use of a current controller introduces problems under light load conditions, which can be an important issue for the vector control of single-phase IMs. The proposed strategy in this paper can be used for 3-phase IMs under an open-phase fault and for single-phase IMs with main and auxiliary windings.

The major contribution of this study is the development of a FOC algorithm for star-connected 3-phase IM drives, which can be used for healthy and faulty (open-circuit fault) 3-phase IMs. The proposed active fault-tolerant control method in this paper does not need a new FOC algorithm when a fault occurs. It is based on the conventional FOC algorithm, which is modified for faulty conditions. It is shown that by switching the motor parameters and using two different unbalanced transformation matrices for the stator current and voltage variables, the vector control of a faulty 3-phase IM is possible. Simulation and experimental results are presented to show the main characteristics of the proposed method and to confirm the methodology and modeling technique used in this paper.

II. Mathematical Model of a Faulty 3-Phase IM

The d-q model of 3-phase IMs under an open-phase fault can be expressed by the following equations (it should be noted that these equations do not depend on which phase of the stator windings is opened; and the modeling of 3-phase IMs under an open-phase fault is fully discussed in [1], [4]):

Stator voltage equations:

TABLE I
The Difference between Model of Healthy and Faulty 3-Phase IM

Faulty 3-Phase IM	Healthy 3-Phase IM
$M_q=\sqrt{3}/2L_{ms}$	$M_q=M=3/2L_{ms}$
$L_{qs}=L_{ls}+1/2L_{ms}$	$L_{qs}=L_s=L_{ls}+3/2L_{ms}$

$$\begin{bmatrix} v_{ds}^s \\ v_{qs}^s \end{bmatrix} = \begin{bmatrix} r_s + L_{ds}p & 0 \\ 0 & r_s + L_{qs}p \end{bmatrix} \begin{bmatrix} i_{ds}^s \\ i_{qs}^s \end{bmatrix} + \begin{bmatrix} M_d p & 0 \\ 0 & M_q p \end{bmatrix} \begin{bmatrix} i_{dr}^s \\ i_{qr}^s \end{bmatrix} \quad (1)$$

Rotor voltages equations:

$$\begin{bmatrix} v_{dr}^s \\ v_{qr}^s \end{bmatrix} = \begin{bmatrix} M_d p & \omega_r M_q \\ -\omega_r M_d & M_q p \end{bmatrix} \begin{bmatrix} i_{ds}^s \\ i_{qs}^s \end{bmatrix} + \begin{bmatrix} r_r + L_r p & \omega_r L_r \\ -\omega_r L_r & r_r + L_r p \end{bmatrix} \begin{bmatrix} i_{dr}^s \\ i_{qr}^s \end{bmatrix} \quad (2)$$

Stator flux equations:

$$\begin{bmatrix} \lambda_{ds}^s \\ \lambda_{qs}^s \end{bmatrix} = \begin{bmatrix} L_{ds} & 0 \\ 0 & L_{qs} \end{bmatrix} \begin{bmatrix} i_{ds}^s \\ i_{qs}^s \end{bmatrix} + \begin{bmatrix} M_d & 0 \\ 0 & M_q \end{bmatrix} \begin{bmatrix} i_{dr}^s \\ i_{qr}^s \end{bmatrix} \quad (3)$$

Rotor flux equations:

$$\begin{bmatrix} \lambda_{dr}^s \\ \lambda_{qr}^s \end{bmatrix} = \begin{bmatrix} M_d & 0 \\ 0 & M_q \end{bmatrix} \begin{bmatrix} i_{ds}^s \\ i_{qs}^s \end{bmatrix} + \begin{bmatrix} L_r & 0 \\ 0 & L_r \end{bmatrix} \begin{bmatrix} i_{dr}^s \\ i_{qr}^s \end{bmatrix} \quad (4)$$

Torque equations:

$$\begin{aligned} T_e &= \frac{pole}{2}\left(M_q i_{qs}^s i_{dr}^s - M_d i_{ds}^s i_{qr}^s\right) \\ T_e - T_l &= \frac{2}{pole}\left(Jp\omega_r + B\omega_r\right) \end{aligned} \quad (5)$$

where:

$$\begin{aligned} &M_d = \frac{3}{2}L_{ms}, M_q = \frac{\sqrt{3}}{2}L_{ms} \\ &L_{ds} = L_{ls} + \frac{3}{2}L_{ms}, L_{qs} = L_{ls} + \frac{1}{2}L_{ms}, p = \frac{d}{dt} \end{aligned} \quad (6)$$

In these equations, v^s_{ds} and v^s_{qs} are the stator d-q axes voltages, i^s_{ds} and i^s_{qs} are the stator d-q axes currents, i^s_{dr} and i^s_{qr} are the rotor d-q axes currents, λ^s_{ds} and λ^s_{qs} are the stator d-q axes fluxes, and λ^s_{dr} and λ^s_{qr} are the rotor d-q axes fluxes in the stationary reference frame (superscript "s"). r_s and r_r indicate the stator and rotor resistances. L_{ds}, L_{qs}, L_r, L_{ms}, M_d and M_q denote the stator and rotor d-q axes self and mutual inductances. ω_r is the motor speed. T_e and T_l are the electromagnetic torque and load torque, J and B are the moment of inertia and the viscous friction coefficient, respectively. As can be seen from (1)-(5), the structure of healthy and faulty 3-phase IMs are the same. Actually, by replacing $M_d=M_q=M=3/2L_{ms}$ and $L_{ds}=L_{qs}=L_s=L_{ls}+3/2L_{ms}$ in the faulty 3-phase IM equations, the equations of healthy IMs are obtained [1], [4]. The differences between the models of healthy and faulty 3-phase IMs are summarized in Table I.

TABLE II
THE COMPARISON BETWEEN EQUATIONS OF FLUX, SPEED AND TORQUE FOR HEALTHY AND FAULTY 3-PHASE IM IN THE ROTATING REFERENCE FRAME

	Healthy IM	Faulty IM [1]	Faulty IM [4]
a_i, b_i, c_i, d_i	$a_i = \cos\theta_{mr}, b_i = \sin\theta_{mr}$ $c_i = -\sin\theta_{mr}, d_i = \cos\theta_{mr}$	$a_i = \frac{M_d}{M_q}\cos\theta_{mr}, b_i = \sin\theta_{mr}$ $c_i = -\frac{M_d}{M_q}\sin\theta_{mr}, d_i = \cos\theta_{mr}$	$a_i = \sqrt{M_d/M_q}\cos\theta_{mr}, b_i = \sqrt{M_q/M_d}\sin\theta_{mr}$ $c_i = -\sqrt{M_d/M_q}\sin\theta_{mr}, d_i = \sqrt{M_q/M_d}\cos\theta_{mr}$
Transformation matrix for stator current variables	$[T_{is}^{mr}] = \begin{bmatrix} \cos\theta_{mr} & \sin\theta_{mr} \\ -\sin\theta_{mr} & \cos\theta_{mr} \end{bmatrix}$	$[T_{is}^{mr}] = \begin{bmatrix} \frac{M_d}{M_q}\cos\theta_{mr} & \sin\theta_{mr} \\ -\frac{M_d}{M_q}\sin\theta_{mr} & \cos\theta_{mr} \end{bmatrix}$	$[T_{is}^{mr}] = \begin{bmatrix} \sqrt{M_d/M_q}\cos\theta_{mr} & \sqrt{M_q/M_d}\sin\theta_{mr} \\ -\sqrt{M_d/M_q}\sin\theta_{mr} & \sqrt{M_q/M_d}\cos\theta_{mr} \end{bmatrix}$
Flux equation	$\lvert\lambda_r\rvert = \frac{Mi_{ds}^{mr}}{1+T_r p}$	$\lvert\lambda_r\rvert = \frac{M_q i_{ds}^{mr}}{1+T_r p}$	$\lvert\lambda_r\rvert = \frac{\sqrt{M_d M_q} i_{ds}^{mr}}{1+T_r p}$
Torque equation	$T_e = \frac{pole}{2}\frac{M}{L_r}\lvert\lambda_r\rvert i_{qs}^{mr}$	$T_e = \frac{pole}{2}\frac{M_q}{L_r}\lvert\lambda_r\rvert i_{qs}^{mr}$	$T_e = \frac{pole}{2}\frac{\sqrt{M_d M_q}}{L_r}\lvert\lambda_r\rvert i_{qs}^{mr}$
Speed equation	$\omega_{mr} = \omega_r + \frac{Mi_{qs}^{mr}}{T_r\lvert\lambda_r\rvert}$	$\omega_{mr} = \omega_r + \frac{M_q i_{qs}^{mr}}{T_r\lvert\lambda_r\rvert}$	$\omega_{mr} = \omega_r + \frac{\sqrt{M_d M_q} i_{qs}^{mr}}{T_r\lvert\lambda_r\rvert}$

III. ROTOR FOC OF 3-PHASE IMS UNDER AN OPEN-PHASE FAULT

Among the various kinds of vector control methods, the FOC method is the most highly adopted method for the high performance control of IMs. In the conventional Rotor FOC (RFOC) the equations of a machine are transformed to the rotating reference frame. The transformation matrix that is used for this purpose is:

$$[T_s^{mr}] = \begin{bmatrix} \cos\theta_{mr} & \sin\theta_{mr} \\ -\sin\theta_{mr} & \cos\theta_{mr} \end{bmatrix} \tag{7}$$

In (7), θ_{mr} is the angle between the stationary reference frame and the rotating reference frame (in this paper the superscript "*mr*" indicates that the variables are in the rotating reference frame). For the unbalanced conditions used in this paper, the conventional transformation matrix can be applied to the rotor variables. However, to overcome the effect of the asymmetrical stator winding structure to obtain a non-pulsating torque, it is necessary to define an unbalanced transformation matrix for stator variables. The reason for using this transformation matrix is to obtain a model of a faulty IM with a balanced structure.

A. Transformation Matrix for Stator Current Variables

A transformation matrix for stator current variables can be considered as:

$$\begin{bmatrix} i_{ds}^{mr} \\ i_{qs}^{mr} \end{bmatrix} = [T_{is}^{mr}] \begin{bmatrix} i_{ds}^{s} \\ i_{qs}^{s} \end{bmatrix} = \begin{bmatrix} a_i & b_i \\ c_i & d_i \end{bmatrix} \begin{bmatrix} i_{ds}^{s} \\ i_{qs}^{s} \end{bmatrix} \tag{8}$$

It can be shown that the structure of the torque equation for a faulty IM can be obtained similar to that of a balanced 3-phase IM torque using two different transformation matrices as presented in [1] and [4]. In [1], the transformation matrix is given by:

$$a_i = \frac{M_d}{M_q}\cos\theta_{mr}, b_i = \sin\theta_{mr}, c_i = -\frac{M_d}{M_q}\sin\theta_{mr}, d_i = \cos\theta_{mr} \tag{9}$$

Meanwhile, in [4], it is given by:

$$\begin{aligned} a_i &= \sqrt{M_d/M_q}\cos\theta_{mr}, b_i = \sqrt{M_q/M_d}\sin\theta_{mr} \\ c_i &= -\sqrt{M_d/M_q}\sin\theta_{mr}, d_i = \sqrt{M_q/M_d}\cos\theta_{mr} \end{aligned} \tag{10}$$

Based on (9) and (10), the transformation matrixes for the stator current variables are obtained as (11) and (12) respectively:

$$\begin{bmatrix} i_{ds}^{mr} \\ i_{qs}^{mr} \end{bmatrix} = [T_{is}^{mr}] \begin{bmatrix} i_{ds}^{s} \\ i_{qs}^{s} \end{bmatrix} = \begin{bmatrix} \frac{M_d}{M_q}\cos\theta_{mr} & \sin\theta_{mr} \\ -\frac{M_d}{M_q}\sin\theta_{mr} & \cos\theta_{mr} \end{bmatrix} \begin{bmatrix} i_{ds}^{s} \\ i_{qs}^{s} \end{bmatrix} \tag{11}$$

$$\begin{aligned} \begin{bmatrix} i_{ds}^{mr} \\ i_{qs}^{mr} \end{bmatrix} &= [T_{is}^{mr}] \begin{bmatrix} i_{ds}^{s} \\ i_{qs}^{s} \end{bmatrix} \\ &= \begin{bmatrix} \sqrt{M_d/M_q}\cos\theta_{mr} & \sqrt{M_q/M_d}\sin\theta_{mr} \\ -\sqrt{M_d/M_q}\sin\theta_{mr} & \sqrt{M_q/M_d}\cos\theta_{mr} \end{bmatrix} \begin{bmatrix} i_{ds}^{s} \\ i_{qs}^{s} \end{bmatrix} \end{aligned} \tag{12}$$

Using (11) and (12) and after simplification, the electromagnetic torque can be obtained as (13) and (14), respectively [1], [4]:

$$T_e = \frac{pole}{2} M_q (i_{qs}^{mr} i_{dr}^{mr} - i_{ds}^{mr} i_{qr}^{mr}) \tag{13}$$

and:

TABLE III
THE COMPARISON BETWEEN EQUATIONS OF STATOR VOLTAGES FOR HEALTHY AND FAULTY 3-PHASE IM IN THE ROTATING REFERENCE FRAME

	Healthy IM	Faulty IM
Stator d-axis voltage equation	$v_{ds}^{mr} = r_s i_{ds}^{mr} + (L_s - \frac{M^2}{L_r}) p i_{ds}^{mr}$ $- \omega_{mr}(L_s - \frac{M^2}{L_r}) i_{qs}^{mr} + (\frac{M}{L_r})(\frac{M i_{ds}^{mr} - \lvert\lambda_r\rvert}{T_r})$	$v_{ds}^{mr} = (\frac{r_s M_q^2 + r_s M_d^2}{2M_d^2}) i_{ds}^{mr} + (L_{qs} - \frac{M_q^2}{L_r}) p i_{ds}^{mr} - \omega_{mr}(L_{qs} - \frac{M_q^2}{L_r}) i_{qs}^{mr}$ $+ (\frac{M_q}{L_r})(\frac{M_q i_{ds}^{mr} - \lvert\lambda_r\rvert}{T_r}) + (\frac{r_s M_q^2 - r_s M_d^2}{2M_d^2})(\cos 2\theta_{mr} i_{ds}^{mr} - \sin 2\theta_{mr} i_{qs}^{mr})$
Stator q-axis voltage equation	$v_{qs}^{mr} = r_s i_{qs}^{mr} + (L_s - \frac{M^2}{L_r}) p i_{qs}^{mr}$ $+ \omega_{mr}(L_s - \frac{M^2}{L_r}) i_{ds}^{mr} + \omega_{mr} M \frac{\lvert\lambda_r\rvert}{L_r}$	$v_{qs}^{mr} = (\frac{r_s M_q^2 + r_s M_d^2}{2M_d^2}) i_{qs}^{mr} + (L_{qs} - \frac{M_q^2}{L_r}) p i_{qs}^{mr} + \omega_{mr}(L_{qs} - \frac{M_q^2}{L_r}) i_{ds}^{mr}$ $+ \omega_{mr} M_q \frac{\lvert\lambda_r\rvert}{L_r} + (\frac{r_s M_q^2 - r_s M_d^2}{2M_d^2})(-\sin 2\theta_{mr} i_{ds}^{mr} - \cos 2\theta_{mr} i_{qs}^{mr})$

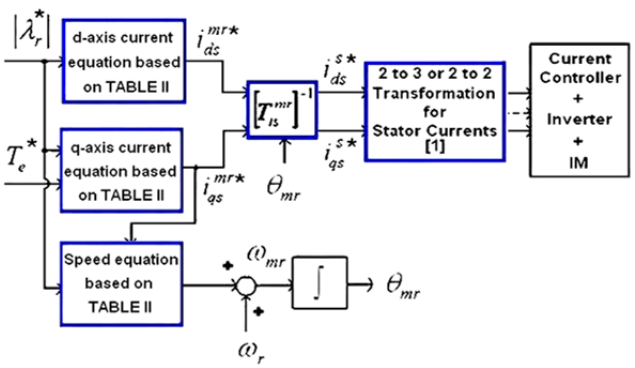

Fig. 2. Current controller block diagram of Indirect RFOC for star-connected 3-phase IM under normal and open-phase fault conditions.

$$T_e = \frac{pole}{2}\sqrt{M_d M_q}\,(i_{qs}^{mr} i_{dr}^{mr} - i_{ds}^{mr} i_{qr}^{mr}) \tag{14}$$

As can be seen, by using (11) and (12), the torque equation of a faulty 3-phase IM becomes similar to that of a healthy 3-phase IM. The only difference between (13) and a healthy 3-phase IM torque equation is that, in (13): M_q=$\sqrt{3}/2L_{ms}$, but in the healthy condition: M=3/2L_{ms}. Moreover, the difference between (14) and a healthy 3-phase IM torque equation is that, in (14): $\sqrt{M_d M_q}$≈1.14L_{ms}, but in the healthy condition: M=3/2L_{ms}. A comparison between the equations of the flux, speed and torque for healthy and faulty 3-phase IMs in the rotating reference frame based on the presented transformation matrices for stator current variables (equation (11) and (12)) is summarized in Table II (to obtain these equations the assumptions λ_{dr}^{mr}=$|\lambda_r|$ and λ_{qr}^{mr}=0 have been considered). In Table II, T_r is the rotor time constant (T_r=L_r/r_r). From the results of Table II, it is possible to adopt the indirect field-oriented control scheme, as shown in Fig. 2, where $|\lambda_r^*|$ and T_e^* represent the reference flux and torque, respectively. In Fig. 2, the blue blocks represent the portions of the conventional FOC that require modifications under faulty conditions.

B. Transformation Matrix for Stator Voltage Variables

Like equation (8), a transformation matrix for the stator voltage variables can be written as:

$$\begin{bmatrix} v_{ds}^{mr} \\ v_{qs}^{mr} \end{bmatrix} = [T_{vs}^{mr}] \begin{bmatrix} v_{ds}^{s} \\ v_{qs}^{s} \end{bmatrix} = \begin{bmatrix} a_v & b_v \\ c_v & d_v \end{bmatrix} \begin{bmatrix} v_{ds}^{s} \\ v_{qs}^{s} \end{bmatrix} \tag{15}$$

Using equation (15), the faulty 3-phase IM stator voltage equation can be written as:

$$[T_{vs}^{mr}] \begin{bmatrix} v_{ds}^{s} \\ v_{qs}^{s} \end{bmatrix} = [T_{vs}^{mr}] \begin{bmatrix} r_s + L_{ds}p & 0 \\ 0 & r_s + L_{qs}p \end{bmatrix} [T_{is}^{mr}]^{-1} [T_{is}^{mr}] \begin{bmatrix} i_{ds}^{s} \\ i_{qs}^{s} \end{bmatrix} + [T_{vs}^{mr}] \begin{bmatrix} M_d p & 0 \\ 0 & M_q p \end{bmatrix} [T_s^{mr}]^{-1} [T_s^{mr}] \begin{bmatrix} i_{dr}^{s} \\ i_{qr}^{s} \end{bmatrix} \tag{16}$$

In equation (16), for the sake of simplicity, (11) (rather than (12)) is used for $[T_{is}^{mr}]$. As a result, equation (16) can be written as:

$$\begin{bmatrix} v_{ds}^{mr} \\ v_{qs}^{mr} \end{bmatrix} = \begin{bmatrix} a_v & b_v \\ c_v & d_v \end{bmatrix} \begin{bmatrix} \frac{M_q}{M_d} r_{ds} \cos\theta_{mr} & \frac{-M_q}{M_d} r_{ds} \sin\theta_{mr} \\ r_{qs} \sin\theta_{mr} & r_{qs} \cos\theta_{mr} \end{bmatrix} \begin{bmatrix} i_{ds}^{mr} \\ i_{qs}^{mr} \end{bmatrix} + \begin{bmatrix} a_v & b_v \\ c_v & d_v \end{bmatrix} \begin{bmatrix} \frac{M_q}{M_d} L_{ds} \cos\theta_{mr} & \frac{-M_q}{M_d} L_{ds} \sin\theta_{mr} \\ L_{qs} \sin\theta_{mr} & L_{qs} \cos\theta_{mr} \end{bmatrix} \begin{bmatrix} pi_{ds}^{mr} \\ pi_{qs}^{mr} \end{bmatrix} + \omega_{mr} \begin{bmatrix} a_v & b_v \\ c_v & d_v \end{bmatrix} \begin{bmatrix} \frac{-M_q}{M_d} L_{ds} \sin\theta_{mr} & \frac{-M_q}{M_d} L_{ds} \cos\theta_{mr} \\ L_{qs} \cos\theta_{mr} & -L_{qs} \sin\theta_{mr} \end{bmatrix} \begin{bmatrix} i_{ds}^{mr} \\ i_{qs}^{mr} \end{bmatrix} + \omega_{mr} \begin{bmatrix} a_v & b_v \\ c_v & d_v \end{bmatrix} \begin{bmatrix} -M_d \sin\theta_{mr} & -M_d \cos\theta_{mr} \\ M_q \cos\theta_{mr} & -M_q \sin\theta_{mr} \end{bmatrix} \begin{bmatrix} i_{dr}^{mr} \\ i_{qr}^{mr} \end{bmatrix} + \begin{bmatrix} a_v & b_v \\ c_v & d_v \end{bmatrix} \begin{bmatrix} M_d \cos\theta_{mr} & -M_d \sin\theta_{mr} \\ M_q \sin\theta_{mr} & M_q \cos\theta_{mr} \end{bmatrix} \begin{bmatrix} pi_{dr}^{mr} \\ pi_{qr}^{mr} \end{bmatrix} \tag{17}$$

assuming that:

$$a_v = -b_v.Z_5.\cot\theta_{mr} \;,\; c_v = d_v.Z_5.\tan\theta_{mr}$$
$$Z_5 = \left(\frac{L_{qs} - \frac{M_q^2}{L_r}}{-\frac{L_{ds}M_q}{M_d} + \frac{M_d M_q}{L_r}} \right) \tag{18}$$

TABLE IV
THE COMPARISON BETWEEN CONVENTIONAL AND PROPOSED VECTOR CONTROL METHODS

	Conventional controller	Proposed controller
3 to 2 or 2 to 2 transformation for the stator currents based on [1], [4]	$\begin{bmatrix} i_{ds}^s \\ i_{qs}^s \end{bmatrix} = \sqrt{\frac{2}{3}} \begin{bmatrix} +1 & -\frac{1}{2} & -\frac{1}{2} \\ 0 & \frac{\sqrt{3}}{2} & -\frac{\sqrt{3}}{2} \end{bmatrix} \begin{bmatrix} i_{as} \\ i_{bs} \\ i_{cs} \end{bmatrix}$	$\begin{bmatrix} i_{ds}^s \\ i_{qs}^s \end{bmatrix} = \frac{\sqrt{2}}{2} \begin{bmatrix} 1 & -1 \\ 1 & 1 \end{bmatrix} \begin{bmatrix} i_{as} \\ i_{bs} \end{bmatrix}$
Rotational transformation matrix for the stator currents based on (11), [1]	$\begin{bmatrix} i_{ds}^{mr} \\ i_{qs}^{mr} \end{bmatrix} = \begin{bmatrix} \cos\theta_{mr} & \sin\theta_{mr} \\ -\sin\theta_{mr} & \cos\theta_{mr} \end{bmatrix} \begin{bmatrix} i_{ds}^s \\ i_{qs}^s \end{bmatrix}$	$\begin{bmatrix} i_{ds}^{mr} \\ i_{qs}^{mr} \end{bmatrix} = \begin{bmatrix} \frac{M_d}{M_q}\cos\theta_{mr} & \sin\theta_{mr} \\ -\frac{M_d}{M_q}\sin\theta_{mr} & \cos\theta_{mr} \end{bmatrix} \begin{bmatrix} i_{ds}^s \\ i_{qs}^s \end{bmatrix}$
Inverse of transformation matrix for the stator voltages based on (20)	$\begin{bmatrix} v_{ds}^s \\ v_{qs}^s \end{bmatrix} = \begin{bmatrix} \cos\theta_{mr} & -\sin\theta_{mr} \\ \sin\theta_{mr} & \cos\theta_{mr} \end{bmatrix} \begin{bmatrix} v_{ds}^{mr} \\ v_{qs}^{mr} \end{bmatrix}$	$\begin{bmatrix} v_{ds}^s \\ v_{qs}^s \end{bmatrix} = \begin{bmatrix} -\cos\theta_{mr} & \sin\theta_{mr} \\ -\frac{M_q}{M_d}\sin\theta_{mr} & -\frac{M_q}{M_d}\cos\theta_{mr} \end{bmatrix} \begin{bmatrix} v_{ds}^{mr} \\ v_{qs}^{mr} \end{bmatrix}$
Stator self and mutual inductance based on Table II, Table III	$L_s = L_{ls} + \frac{3}{2}L_{ms}, M = \frac{3}{2}L_{ms}$	$L_{qs} = L_{ls} + \frac{1}{2}L_{ms}, M_q = \frac{\sqrt{3}}{2}L_{ms}$
Stator resistance based on Table III	r_s	$\frac{r_s M_q^2 + r_s M_d^2}{2M_d^2} = \frac{2}{3}r_s$
Extra terms in the stator voltage equations based on Table III	----------	$\begin{bmatrix} v_{ds}^{et} \\ v_{qs}^{et} \end{bmatrix} = \left(\frac{r_s M_q^2 - r_s M_d^2}{2M_d^2}\right) \begin{bmatrix} i_{ds}^{et} \\ i_{qs}^{et} \end{bmatrix} = -\frac{r_s}{3} \begin{bmatrix} i_{ds}^{et} \\ i_{qs}^{et} \end{bmatrix}$ $\begin{bmatrix} i_{ds}^{et} \\ i_{qs}^{et} \end{bmatrix} = \begin{bmatrix} \cos 2\theta_{mr} & -\sin 2\theta_{mr} \\ -\sin 2\theta_{mr} & -\cos 2\theta_{mr} \end{bmatrix} \begin{bmatrix} i_{ds}^{mr} \\ i_{qs}^{mr} \end{bmatrix}$

The faulty 3-phase IM stator voltage equations are obtained similar to the balanced 3-phase IM stator voltage equations. As a result, a_v, b_v, c_v and d_v can be considered as:

$$a_v = -\cos\theta_{mr}\,, b_v = \left(\frac{-L_{ds}L_r M_q + M_d^2 M_q}{L_{qs}L_r M_d - M_d M_q^2}\right)\sin\theta_{mr}$$
$$c_v = \sin\theta_{mr}\ ,\quad d_v = \left(\frac{-L_{ds}L_r M_q + M_d^2 M_q}{L_{qs}L_r M_d - M_d M_q^2}\right)\cos\theta_{mr} \tag{19}$$

Based on (19) and by considering $(M_d/M_q)^2=L_{ds}/L_{qs}$, the proposed transformation matrix for the stator voltage variables is obtained as (20) (in a 3-phase IM under open-phase fault: $M_q=\sqrt{3}/2L_{ms}$, $M_d=3/2L_{ms}$, $L_{qs}=L_{ls}+1/2L_{ms}$, $L_{ds}=L_{ls}+3/2L_{ms}$, and $L_{ms}>>L_{ls}$. Therefore, the assumption $L_{qs}/L_{ds}=(M_q/M_d)^2$ is valid).

$$\begin{bmatrix} v_{ds}^{mr} \\ v_{qs}^{mr} \end{bmatrix} = \left[T_{vs}^{mr}\right] \begin{bmatrix} v_{ds}^s \\ v_{qs}^s \end{bmatrix} = \begin{bmatrix} -\cos\theta_{mr} & -\frac{M_d}{M_q}\sin\theta_{mr} \\ \sin\theta_{mr} & -\frac{M_d}{M_q}\cos\theta_{mr} \end{bmatrix} \begin{bmatrix} v_{ds}^s \\ v_{qs}^s \end{bmatrix} \tag{20}$$

Using (20), it is expected that the stator voltage equations of a faulty motor in the rotating reference frame will become similar to the healthy 3-phase IMs stator voltage equations. A comparison between the equations of the stator voltages for healthy and faulty 3-phase IMs is given in Table III. As can be seen from Table III, the structures of the stator voltage equations for healthy and faulty 3-phase IMs are similar. The difference is in the parameters ($r_s \rightarrow r_s M_q^2 + r_s M_d^2/2M_d^2$, $M \rightarrow M_q$ and $L_s \rightarrow L_{qs}$). It is also noted that the stator voltage equations of a faulty machine contain the extra terms:

$$v_{ds}^{et} = \left(\frac{r_s M_q^2 - r_s M_d^2}{2M_d^2}\right)(\cos 2\theta_{mr} i_{ds}^{mr} - \sin 2\theta_{mr} i_{qs}^{mr}) \tag{21}$$

$$v_{qs}^{et} = \left(\frac{r_s M_q^2 - r_s M_d^2}{2M_d^2}\right)(-\sin 2\theta_{mr} i_{ds}^{mr} - \cos 2\theta_{mr} i_{qs}^{mr}) \tag{22}$$

A comparison between the equations of the RFOC of a faulty 3-phase IM using the proposed method and the equations of the RFOC for a healthy 3-phase IM is summarized in Table IV.

Finally, based on Table II, Table III and Table IV, the proposed vector control of a 3-phase IM under normal and open-phase fault conditions can be constructed as shown in Fig. 3. In this figure, the blue blocks show the modifications needed for the conventional vector control so that it can be applied to a faulty 3-phase IM.

IV. SIMULATION RESULTS

To show the dynamic behavior of a 3-phase IM under an open-phase fault, simulations are conducted using MATLAB (M-File) software. The model of a faulty IM (equations (1)-(6)) assumes a connection between the neutral of the star connected IM machine and the mid-point of the DC link voltage. The

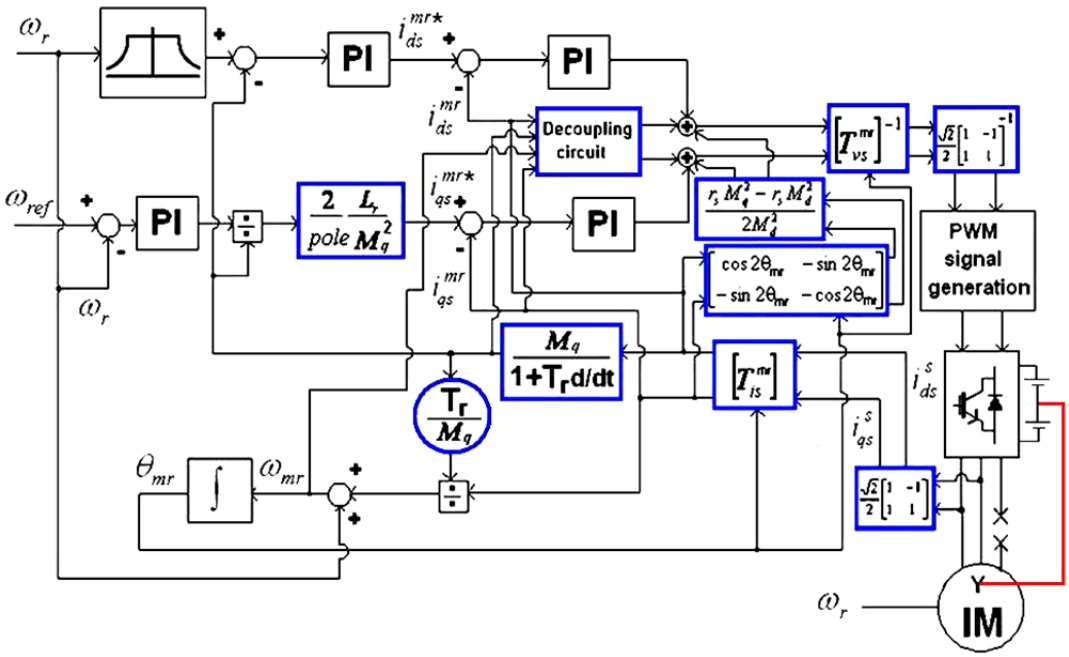

Fig. 3. Block diagram of the proposed IRFOC for star-connected 3-phase IM under normal and open-phase fault conditions.

reason for using M-File instead the IM model from SimPowerSystem provided with MATLAB is that the neutral point of the IM in SimPowerSystem is not accessible. As a result, it cannot be used to model the faulty IM applied in this paper. The parameters of the simulated IM are listed in the Appendix. The fourth order Runge-Kutta algorithm has been used to solve the healthy and faulty IM equations.

Fig. 4 shows the results obtained from the simulation of a 3-phase IM which is directly connected to a balanced 3-phase power supply. From t=0s to t=10s, the IM runs in the healthy mode and the motor is modeled using healthy 3-phase IM equations. At t= 10s, an open-phase fault is introduced in phase "c". As a result, at t≥10s, the motor is simulated using the faulty machine equations given by (1)-(6).

As can be seen from Fig. 4, a significant amount of oscillations appear in the torque, and hence speed, right after the open-phase fault is introduced. The oscillations in the torque are due to the unbalanced structure of the IM, mainly in its d and q inductances. Due to the connection between the neutral point of the stator and the neutral point of the supply, independent currents flow in the remaining phases as can be seen in Figure 4(d).

V. Experimental Results

To study the performances of the conventional and proposed methods for the vector control of healthy and faulty 3-phase IMs, a prototype of a star-connected 3-phase IM drive was built in the laboratory. Experimental tests were carried out based on Fig. 3. The scheme used for the experimental setup is shown in Fig. 5.

This paper investigates the use of the scheme shown in Fig. 5 for feeding a 3-phase IM under an open-phase fault. Two large capacitors are connected in series between the positive and negative rails of the DC link voltage in order to create a mid-point DC link voltage. When an open-phase fault occurs in one of the phases, the remaining two phases can only be controlled independently if the neutral point of the IM is connected to the mid-point of the DC link (as indicated in Fig. 5). During healthy mode operation, the 3-phase machine is fed with PWM voltage generated by the FOC controller. In the healthy mode, the stator current that flows in the neutral wire is very small due to the PWM operation of the inverter [21]. This paper considers the use of the simple topology shown in Fig.5. It should be emphasized that the focuse is not on the topology but on the analysis, design and implementation of the vector control strategy based FOC for a star-connected 3-phase IM drive under an open-phase fault.

A photograph of the developed experimental rig is shown in Fig. 6, where the 3-phase IM is supplied by a 3-phase IGBT Voltage Source Inverter (VSI). To emulate the fault condition, an electronic switch is connected in series with phase "c" and it is opened to achieve the faulty condition. A torque transient is expected due to the high di/dt in phase "c" where it is cut-off. The high di/dt also causes a large induced voltage across the inductances and a subsequently high voltage across the switches. To prevent the large induced voltages due to a high di/dt at the instant of a fault, the phase can be opened at the zero crossing as in [21]. However, in practice, an open phase fault can occur at any time (and at any current level). As a result, an electrical arc temporarily presents at the instant of an open phase fault. However, it is not within the scope of this paper to suppress this high voltage transient. In the experimental, simple RC snubber circuits are employed for

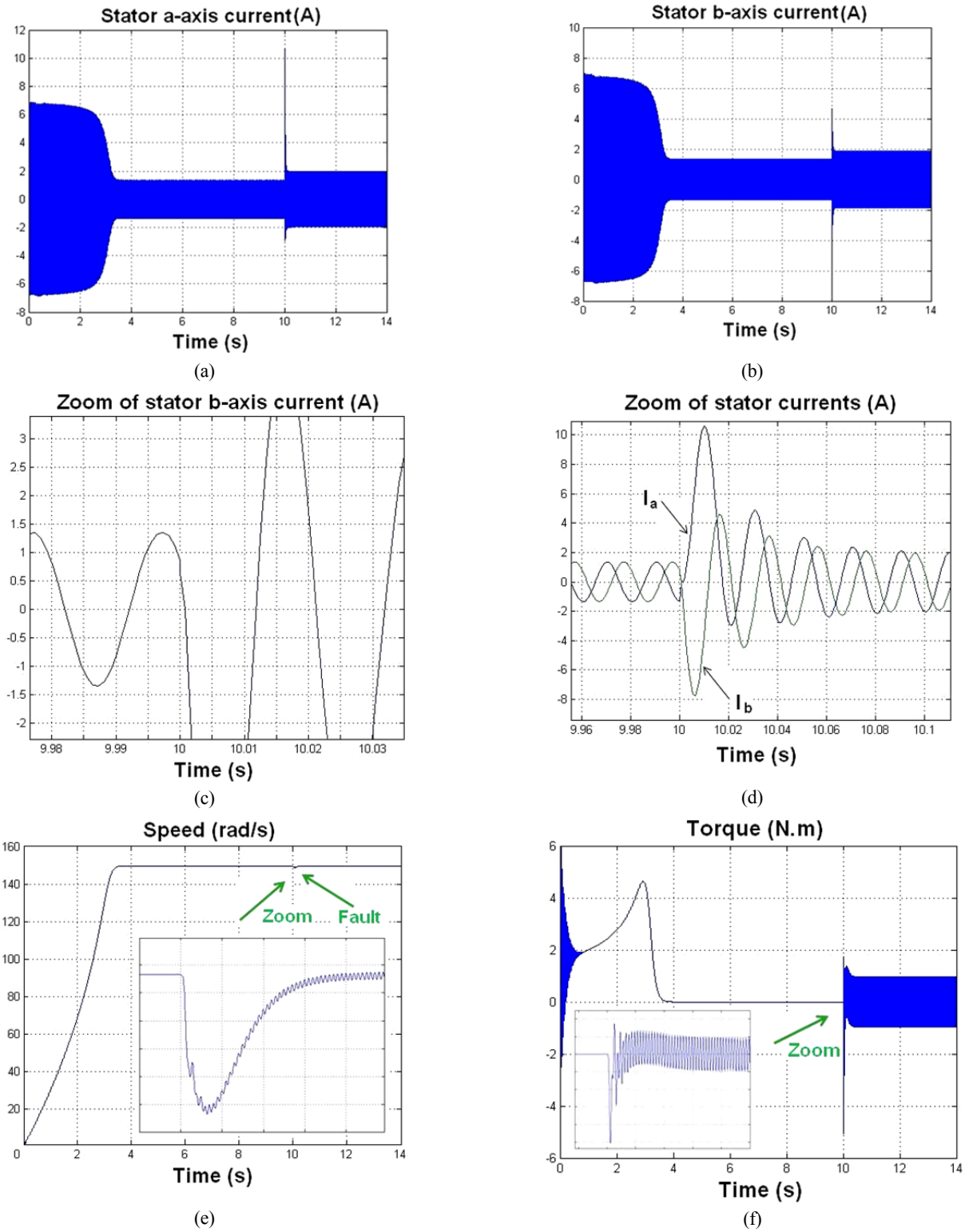

Fig. 4. Simulation results of dynamic behavior of 3-phase IM under normal and open-phase fault operating conditions. (a) Stator a-axis current. (b) Stator b-axis current. (c) Zoom of stator b-axis current. (d) Zoom of stator currents. (e) Speed. (f) Torque.

high voltage protection. A DC voltage of 240V is used for the DC link, and two Hall effect sensors and an incremental encoder are used to measure the stator phase currents and rotor speed, respectively. An open-phase fault is introduced in phase "c" of the stator windings. Therefore, the two sensors are placed in phases "a" and "b" (in practice three sensors should be used since the faulty phase is not known). The code is automatically generated using MATLAB/SIMULINK. Then it

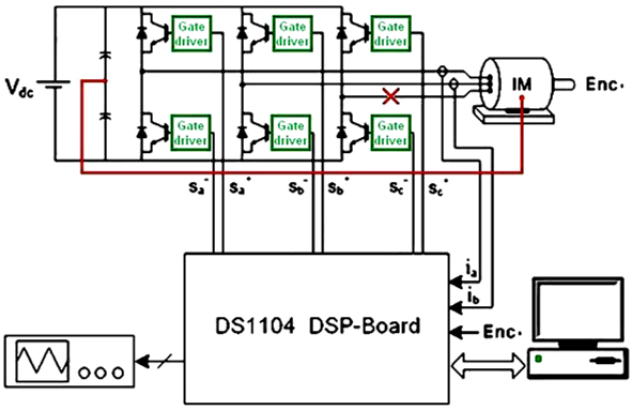

Fig. 5. Scheme used for experimental setup.

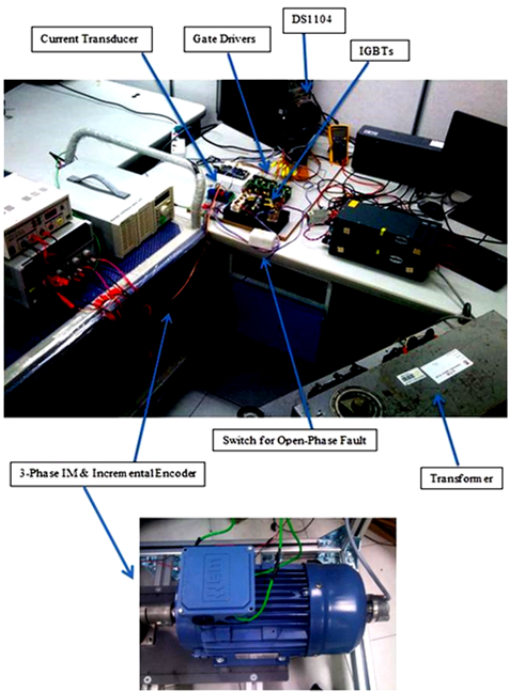

Fig. 6. Photograph of the experimental system.

is downloaded to a dSPACE DS1104 real-time R&D controller board. To generate the PWM signals, a sinusoidal PWM method with a switching frequency of 10kHz with a dead time of 2μs is used. The sampling time of the control algorithm is 200μs.

The conventional and proposed control strategies for both healthy and faulty 3-phase IMs, are individually tested under the same conditions to obtain proper comparison results (the conventional IRFOC method based voltage controller is fully discussed in [22]). The parameters of the star-connected 3-phase IM are given in the Appendix. In order to verify the proposed fault-tolerant control strategy, several experiments are conducted as follows.

A. No-Load Condition

To confirm the effectiveness of the proposed control strategy under the no-load condition, two tests were performed. In the first test (Fig. 7), the 3-phase IM is started under normal conditions and then a phase cut-off is applied at 20.3s. In the second test (Fig. 8), the 3-phase IM is started under normal conditions and then a phase cut-off is applied at 21.4s. In the first test, the conventional FOC is applied throughout the duration of the text. However, for the second test, the proposed FOC (as outline in Table IV) is applied immediately after the fault (instantaneous fault detection is assumed; the fault detection in this paper is based on a comparison between the real speed and the reference speed). In Fig. 7 and Fig. 8 the reference speed during an open-phase fault is changed from 55rad/s to 60rad/s. Moreover, the reference rotor flux is kept constant at the nominal value of 1Wb. Throughout the experiment, the torque during the healthy and faulty conditions is estimated based on the equations given in Table II.

As shown in Fig. 7 and Fig. 8, during the fault condition, the proposed algorithm exhibits good tracking error performances and a faster response when compared to the conventional FOC. As can be seen from Fig. 8, the proposed FOC method produces a smaller torque and fewer speed ripples compared to the conventional FOC method (Fig. 7). From the zoomed in torque response of Fig. 7 and Fig. 8 it can be seen that the ripple of the conventional technique is almost 4N.m. Meanwhile, for the proposed FOC, the ripple is around 2N.m (in this test the ripple of the FOC technique for a healthy machine is almost 0.6N.m). In addition, it is noted that when using the proposed controller, the time to reach the steady-state is shorter than with the conventional controller. As can be seen, the time to reach the steady-state using the conventional controller is about 2.5s, whereas the time to reach steady-state using the proposed controller is about 2s. It can be seen that when compared with proposed controller, the conventional controller is not able to provide such a desired performance due to the unbalance structure of the faulty IM.

Although the conventional and proposed schemes are both able to almost control the star-connected 3-phase IM, in general, the proposed vector control drive system provides a faster response and a better steady-state performance especially in decreasing speed and torque oscillations.

B: Load Condition

Fig. 9 shows experimental results of the proposed FOC applied to an open-phase fault IM under the loaded condition. The motor is operated at a steady speed of 55rad/s and a step load torque of 1.5N.m is applied at 29s (the limitation of the maximum permissible torque for a star-connected 3-phase IM during an open-phase fault is about 38% of the rated torque [23]). Fig. 9(a) shows the reference and actual (measured) rotor speed signals, and Fig. 9(b) shows the applied load step and torque response. As can be seen from Fig. 9, the torque of the faulty machine increases according to the applied load disturbance. Moreover, after a slight disturbance, the speed recovered to the reference speed of 55rad/s. With the proposed

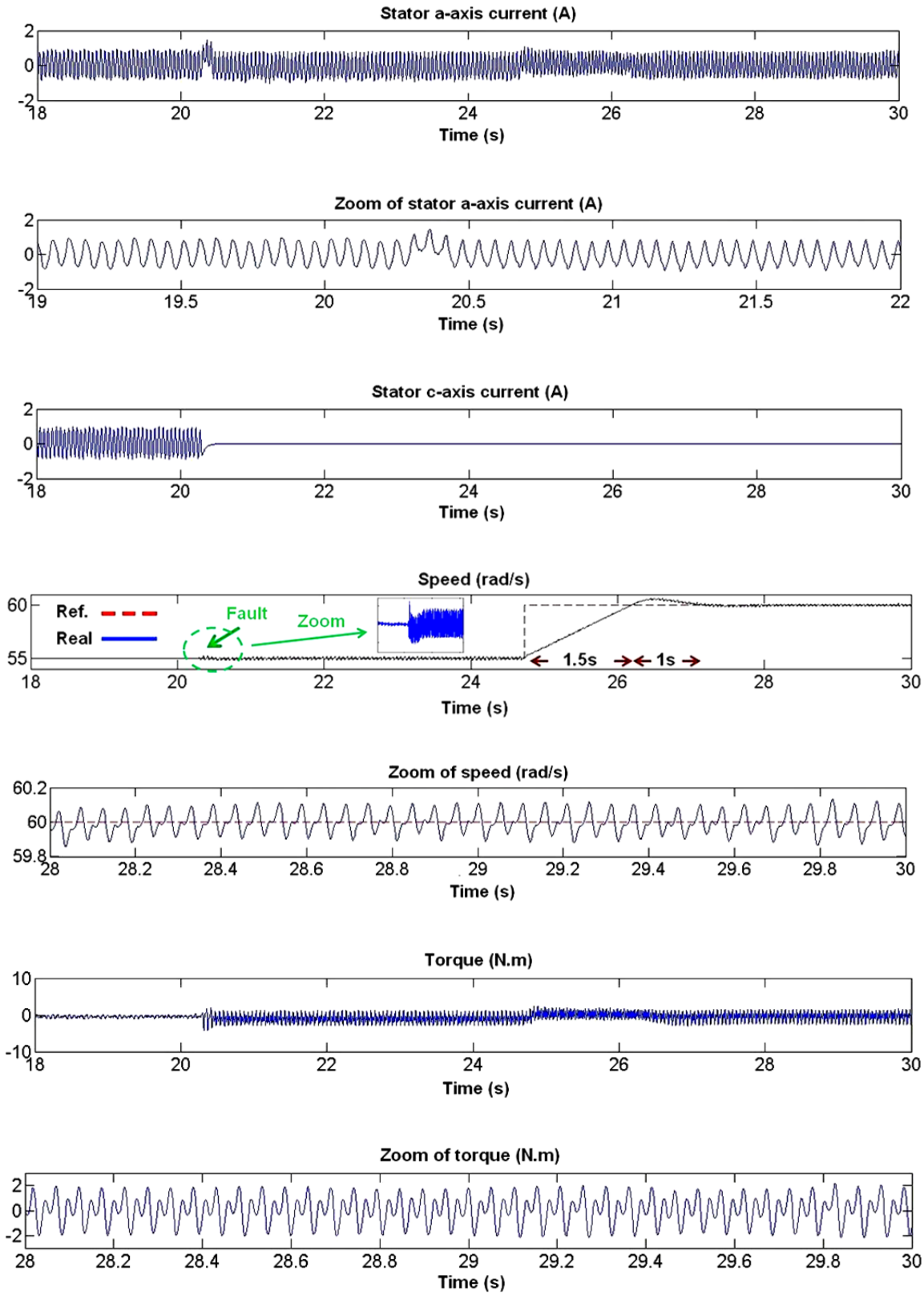

Fig. 7. Experimental results of the conventional IRFO controller from top to bottom: Stator a-axis current, Zoom of stator a-axis current, Stator c-axis current, Speed, Zoom of speed, Torque, Zoom of torque.

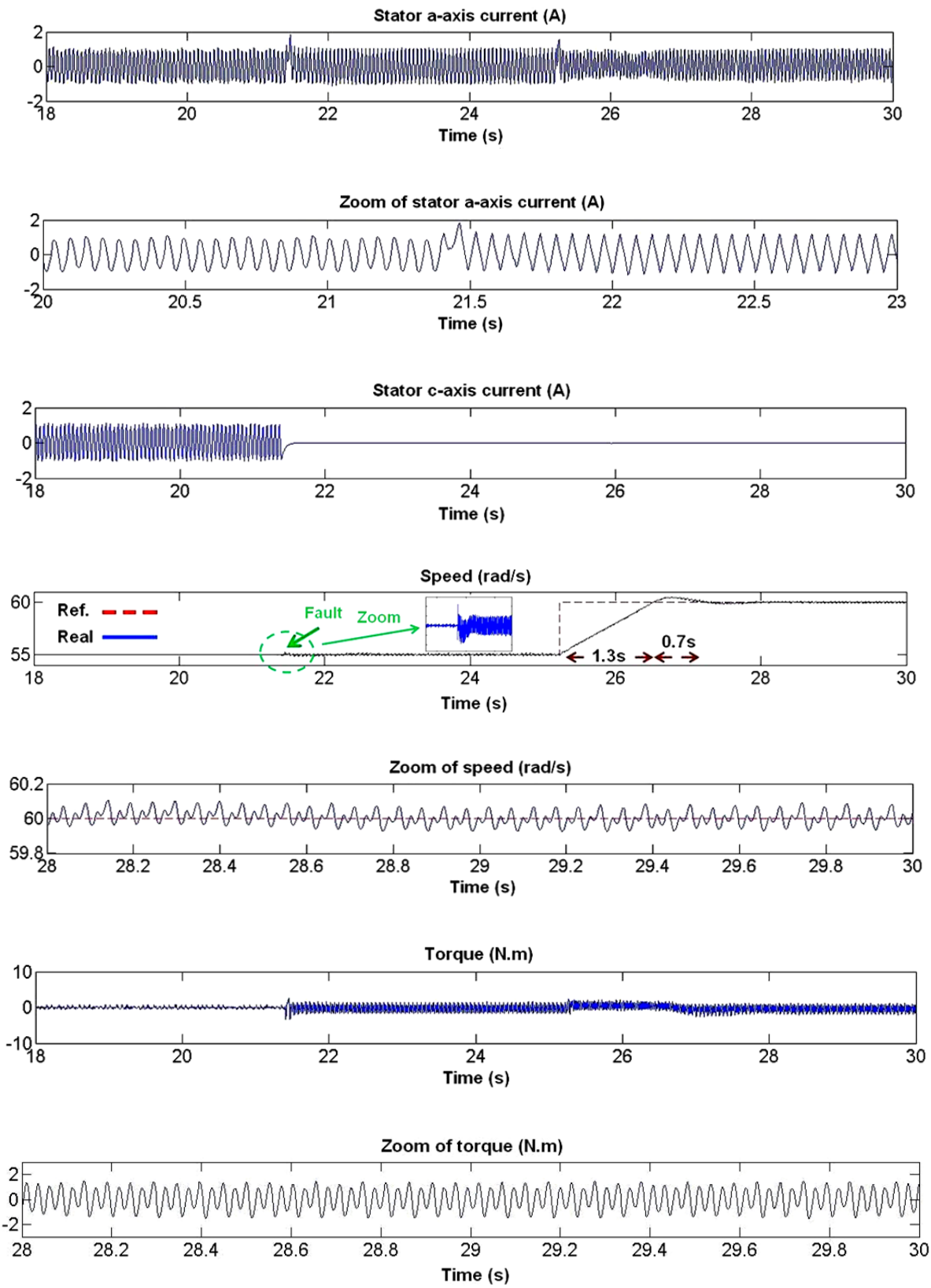

Fig. 8. Experimental results of the proposed IRFO controller from top to bottom: Stator a-axis current, Zoom of stator a-axis current, Stator c-axis current, Speed, Zoom of speed, Torque, Zoom of torque.

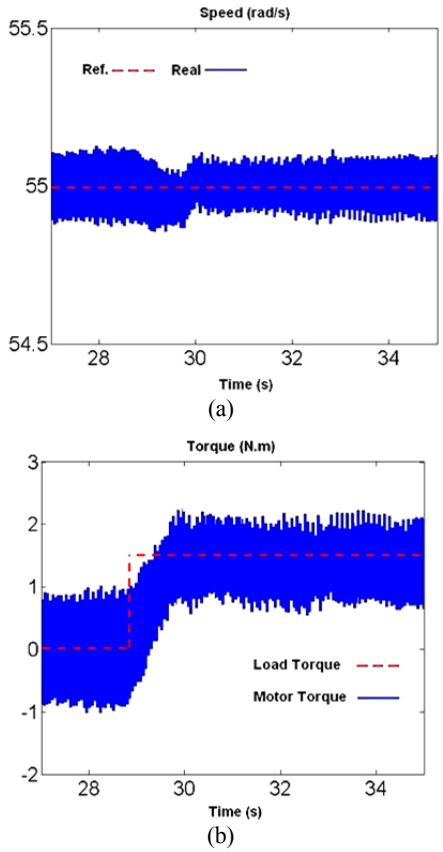

Fig. 9. Experimental results of the proposed IRFO controller during load condition. (a) Speed. (b) Torque.

FOC controller, the torque oscillation of the faulty machine of about 2N.m is recorded before and after the load disturbance is introduced. It can be seen that the rotor speed signal closely follows the reference speed before and after the load disturbance.

In this paper, the vector control of a star-connected 3-phase IM under an open-phase fault is implemented with some minor changes to the conventional FOC strategy. These are changes to the transformation matrices, motor parameters and PI controller coefficients. It should be noted that the PI controller coefficients significantly affect the accuracy of the proposed RFOC method and subsequently the dynamics of the drive system. In this paper, the gains of the PI controllers during healthy and faulty conditions are obtained based on the trial-and-error process. A further investigation on the optimum selection of the gains for the PI controllers has to be carried out to improve the performance of the open-phase fault IM.

VI. Conclusion

This paper presented a fault-tolerant control strategy based on FOC for the high performance vector control of a star-connected 3-phase IM drive. It is shown that with some modifications, it is possible to apply the conventional FOC algorithm to 3-phase IMs under an open-phase fault. The proposed fault-tolerant control method is based on transformation matrices that are used to obtain a model of a faulty IM with a balanced structure. The proposed FOC of a faulty 3-phase IM drive under an open-phase fault can also be applied to a single-phase IM with two windings (main and auxiliary windings). Compared with the conventional FOC, the modified FOC algorithm has managed to reduce the torque and speed oscillations. In addition, it has also managed to improve the dynamic response. Simulation and experimental results are used to validate the effectiveness of the proposed controller.

Appendix

The ratings and parameters of a 3-phase IM:
Power: 1.5kW, V=400V, f=50Hz, poles=4, r_s=5.5Ω, r_r=4.51Ω, M=0.292H, L_s=L_r=0.3065H, J=0.0086kg.m^2

Acknowledgment

The authors would like to thank the Universiti Teknologi Malaysia (UTM) (Q.J130000.2523.12H30) and the Ministry of Education of the Malaysian government for providing the funding for this research.

References

[1] M. Jannati, N. R. N. Idris, and Z. Salem, "A new method for modeling and vector control of unbalanced induction motors," in *Energy Conversion Congress and Exposition (ECCE)*, pp. 3625-3632, Sep. 2012.

[2] M. Jannati, N. R. N. Idris, and M. J. A. Aziz, "A new method for RFOC of Induction Motor under open-phase fault," in *39th Annual Conference on IEEE Industrial Electronics Society, IECON 2013*, pp. 2530-2535, Nov. 2013.

[3] A. Sayed-Ahmed and N. A. Demerdash, "Fault-tolerant operation of delta-connected scalar-and vector-controlled AC motor drives," *IEEE Trans. Power Electron.*, Vol. 27, No. 6, pp. 3041-3049, Jun. 2012.

[4] Z. Yifan and T. A. Lipo, "An approach to modeling and field-oriented control of a three phase induction machine with structural imbalance," in *Proc. APEC, San Jose, TX*, pp. 380-386, Mar. 1996.

[5] M. E. H. Benbouzid, D. Diallo, and M. Zeraoulia, "Advanced fault-tolerant control of induction-motor drives for EV/HEV traction applications: From conventional to modern and intelligent control techniques," *IEEE Trans. Veh. Technol.*, Vol. 56, No. 2, pp. 519-528, Mar. 2007.

[6] D. Kastha and A. K. Majumdar, "An improved starting strategy for voltage-source inverter fed three-phase induction motor drives under inverter fault conditions," *IEEE Trans. Power Electron.*, Vol. 15, No. 4, pp. 726-732, Jul. 2000.

[7] F. Zidani, d. Diallo, M. E. H. Benbouzid, and R. Nait-said, "A fuzzy-based approach for the diagnosis of fault modes in a voltage-fed PWM inverter induction motor drive," *IEEE Trans. Ind. Electron.*, Vol. 55, No. 2, pp. 586-593, Feb. 2008.

[8] A. Raisemche, B. Boukhnifer, C. Larouci, and D. Diallo,

"Two active fault tolerant control schemes of induction motor drive in EV or HEV," *IEEE Trans. Veh. Technol.*, Vol. 63, No. 1, pp. 19-29, Jan. 2014.

[9] C. C. Yeh and N. A. Demerdash, "Fault-tolerant soft starter control of induction motors with reduced transient torque pulsations," *IEEE Trans. Energy Convers.*, Vol. 24, No. 4, pp. 848-859, Dec. 2009.

[10] Z. Liu, X. Yin, Z. Zhang, D. Chen, and W. Chen, "Online rotor mixed fault diagnosis way based on spectrum analysis of instantaneous power in squirrel cage induction motors," *IEEE Trans. Energy Convers.*, Vol. 19, No. 3, pp. 485-490, Sep. 2004.

[11] J. Faiz, V. Ghorbanian, and B. M. Ebrahimi, "EMD-based analysis of industrial induction motors with broken rotor bar for identification of operating point at different supply modes," *IEEE Trans. Ind. Informat.*, Vol. 10, No. 2, pp. 957-966, May 2014.

[12] H. Niemann and J. Stoustrup, "Passive fault tolerant control of a double inverted pendulum – A case study," *Control Engineering Practice*, Vol. 13, No. 8, pp. 1047-1059, Aug. 2005.

[13] R. Oubellil and M. Boukhnifer, "Passive fault tolerant control design of energy management system for electric vehicle," *in 23rd International Symposium on Industrial Electronics (ISIE)*, pp. 1402-1408, Jun. 2014.

[14] M. Salehifar, R. S. Arashloo, M. M. Eguilaz, and V. Sala, "FPGA based robust open transistor fault diagnosis and fault tolerant sliding mode control of five-phase PM motor drives," *Journal of Power Electronics*, Vol. 15, No. 1, pp. 131-145, Jan. 2015.

[15] H. Guzman, M. J. Duran, F. Barrero, B. Bogado, and S. Toral, "Speed control of five-phase induction motors with integrated open-phase fault operation using model-based predictive current control techniques," *IEEE Trans. Ind. Electron.*, Vol. 61, No. 9, pp. 4474-4484, Sep. 2014.

[16] H. M. Ryu, J.-W. Kim, and S.-K. Sul, "Synchronous-frame current control of multiphase synchronous motor under asymmetric fault condition due to open phases," *IEEE Trans. Ind. Appl.*, Vol. 42, No. 4, pp. 1062-1070, Jul./Aug. 2006.

[17] A. Gaeta, G. Scelba, and A. Consoli, "Modeling and control of three-phase PMSMs under open-phase fault," *IEEE Trans. Ind. Appl.*, Vol. 49, No. 1, pp. 74-83, Jan./Feb. 2013.

[18] D. K. Kastha and B. K. Bose, "Fault mode single-phase operation of a variable frequency induction motor drive and improvement of pulsating torque characteristics," *IEEE Trans. Ind. Electron.*, Vol. 41, No. 4, pp. 426-433, Aug. 1994.

[19] D. K. Kastha and B. K. Bose, "On-line search based pulsating torque compensation of a fault mode single-phase variable frequency induction motor drive," *IEEE Trans. Ind. Appl.*, Vol. 31, No. 4, pp. 802-811, Jul./Aug. 2005.

[20] A. Sayed-Ahmed, B. Mirafzal, and N. A. O. Demerdash, "Fault-tolerant technique for Δ-connected AC-motor drives," *IEEE Trans. Energy Convers.*, Vol. 26, No. 2, pp. 646-653, Jun. 2011.

[21] T. H. Liu, J.-R. Fu, and T. A. Lipo, "A strategy for improving reliability of field-oriented controlled induction motor drives," *IEEE Trans. Ind. Appl.*, Vol. 29, No. 5, pp. 910-918, Sep. 1993.

[22] P. Vas, *Vector Control of AC Machines*, Clarendon press Oxford, 1990.

[23] A. Saleh, M. Pacas, and A. Shaltout, "Fault tolerant field oriented control of the induction motor for loss of one inverter phase," in *32nd Annual Conference on IEEE Industrial Electronics*, pp. 817-822, Nov. 2006.

Mohammad Jannati received his B.S. degree in Electrical Engineering from the University of Mazandaran, Babolsar, Iran, in 2008; and his M.S. degree in Electrical Engineering from the University of Guilan, Rasht, Iran, in 2010. He is presently working towards his Ph.D. degree in Electrical Engineering at the Universiti Teknologi Malaysia (UTM), Kuala Lumpur, Malaysia. His current research interests include the control of AC drives.

Nik Rumzi Nik Idris received his B.S. degree in Electrical Engineering from the University of Wollongong, Wollongong, NSW, Australia, in 1989; his M.S. degree in Power Electronics from Bradford University, West Yorkshire, England, UK, in 1993; and his Ph.D. degree from the Universiti Teknologi Malaysia (UTM), Kuala Lumpur, Malaysia, in 2000. He is currently working as an Associate Professor at the UTM. He is presently serving as a Chair for the Power Electronics Chapter of the IEEE Malaysia Section. His current research interests include the control of ac drive systems and DSP applications in power electronic systems.

Mohd Junaidi Abdul Aziz was born in Kuala Terengganu, Malaysia, in 1979. He received his B.S. and M.S. degrees in Electrical Engineering from the Universiti Teknologi Malaysia (UTM), Kuala Lumpur, Malaysia, in 2000 and 2002, respectively; and his Ph.D. in Electrical Engineering from The University of Nottingham, Nottingham, England, UK, in 2008. Since 2008, he has been with the Faculty of Electrical Engineering, UTM, where he is presently a Senior Lecturer. His current research interests include power electronics and electric vehicles with a special focus on battery management systems.